

# Pharmacological Evaluation of Novel Bioisosteres of an Adamantanyl Benzamide P2X<sub>7</sub> Receptor Antagonist.

Shane M. Wilkinson,<sup>†</sup> Melissa L. Barron,<sup>‡</sup> James O'Brien-Brown,<sup>†</sup> Bieneke Janssen,<sup>§</sup> Leanne Stokes,<sup>††</sup> Eryn L. Werry,<sup>‡</sup> Mansoor Chishty,<sup>‡‡</sup> Kristen K. Skarratt,<sup>§§</sup> Jennifer A. Ong,<sup>†††</sup> David E. Hibbs,<sup>†††</sup> Danielle J. Vugts,<sup>§</sup> Stephen Fuller,<sup>§§</sup> Albert D. Windhorst,<sup>§</sup> Michael Kassiou\*.<sup>†</sup>

<sup>†</sup> School of Chemistry, The University of Sydney, NSW 2006 (Australia)

<sup>‡</sup> Faculty of Health Sciences, The University of Sydney, NSW 2006 (Australia)

<sup>§</sup> Department of Radiology & Nuclear Medicine, VU University Medical Center, Amsterdam, De Boelelaan 1117 (The Netherlands)

<sup>††</sup> School of Pharmacy, University of East Anglia, Norwich, NR4 7TJ (UK)

<sup>‡‡</sup> Pharmidex, 14 Hanover St, Mayfair, London W1S 1YH (UK)

<sup>§§</sup> Sydney Medical School Nepean, The University of Sydney, NSW 2006 (Australia)

<sup>†††</sup> Faculty of Pharmacy, The University of Sydney, NSW 2006 (Australia)

**Keywords:** P2X<sub>7</sub>, bioisostere, central nervous system (CNS), pharmacokinetic, metabolism, single nucleotide polymorphisms (SNPs)

**ABSTRACT:** Adamantanyl benzamide **1** was identified as a potent, P2X<sub>7</sub>R antagonist but failed to progress further due to poor metabolic stability. We describe the synthesis and SAR of a series of bioisosteres of benzamide **1** to explore improvements in the pharmacological properties of this lead. Initial efforts investigated a series of heteroaromatic bioisosteres which demonstrated improved physicochemical properties but reduced P2X<sub>7</sub>R antagonism. Installation of bioisosteric fluorine on the adamantane bridgeheads was well tolerated and led to a series of bioisosteres with improved physicochemical properties and metabolic stability. Trifluorinated benzamide **34** demonstrated optimal physicochemical parameters, superior metabolic stability (ten times longer than lead benzamide **1**), an improved physicochemical profile and proved effective in the presence of several known P2X<sub>7</sub>R polymorphisms.

The P2X<sub>7</sub> purinoreceptor (P2X<sub>7</sub>R) is a non-selective, ligand-gated cation channel ubiquitously expressed on many immune cells including microglial cells in the Central Nervous System (CNS). It is up-regulated in response to pro-inflammatory stimuli and has been implicated in a number of neuroinflammatory diseases. Activation of the P2X<sub>7</sub>R by the extracellular nucleotide adenosine triphosphate (ATP) mediates the processing and release of the pro-inflammatory cytokine, interleukin 1 $\beta$  (IL-1 $\beta$ ), which is involved in a variety of cellular actions, including cell proliferation, differentiation, and apoptosis. Additionally, pharmacological inhibition and genetic studies of the P2X<sub>7</sub>R have shown elimination or reduction of symptoms in animal models of arthritis, depression, neuropathic pain, multiple sclerosis, and Alzheimer's disease.<sup>1</sup> The modulation of P2X<sub>7</sub>R activity through the development of P2X<sub>7</sub>R antagonists appears to be a viable strategy for the treatment of neuroinflammatory diseases.

Numerous drug classes have been identified in the pursuit to discover selective P2X<sub>7</sub>R antagonists.<sup>2</sup> Of this diverse library, only a handful have proceeded to clinical trials (Figure 1).<sup>3</sup> Of this list, all disclosed compounds belong to the carboxamide class of P2X<sub>7</sub>R antagonists whereby an aryl group is linked to a cycloalkyl group by

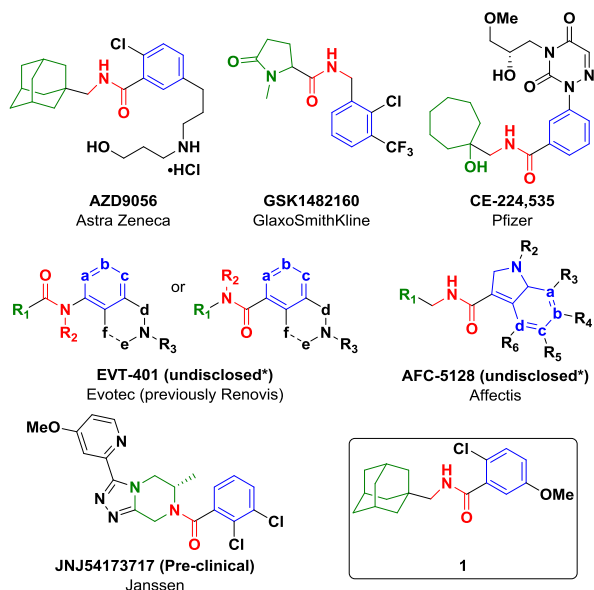


**Figure 1. P2X<sub>7</sub>R antagonists entering clinical trials and adamantanyl benzamide **1**.** The cycloalkyl group, carboxamide linker and aryl moiety are highlighted in green, red and blue respectively. \*Undisclosed structures are speculative based on filed patents.

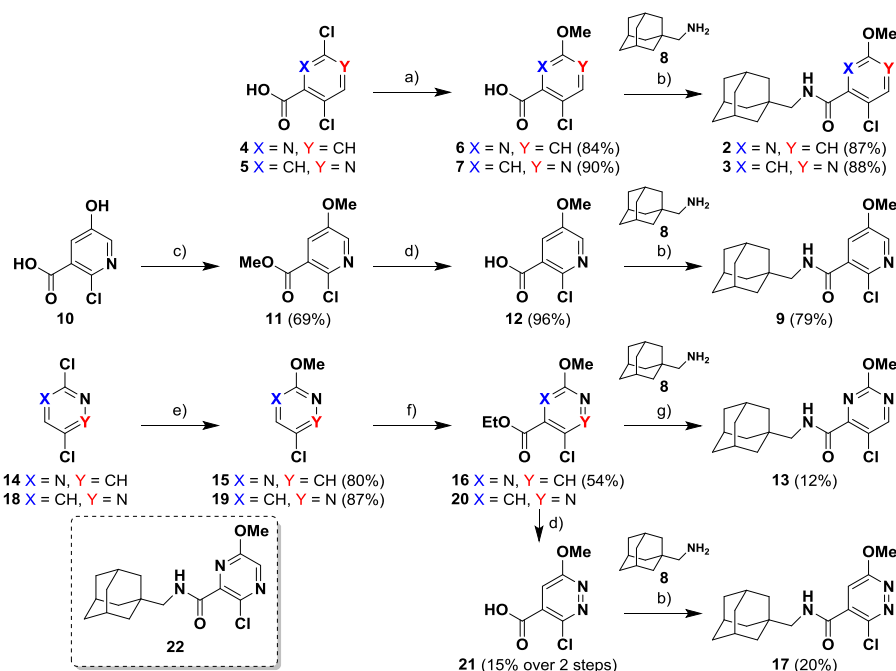
a carboxamide linker. These compounds appear to be evolutionary from a series of potent carboxamides first reported by AstraZeneca<sup>4</sup>. Unfortunately, these initial carboxamides (such as adamantanyl benzamide **1**) were reported to have low metabolic stability. Consequently, we and others have comprehensively explored the chemical space around AstraZeneca's adamantanyl benzamide series in the hope of improving the activity and ADMET properties of this series.

Several structure-activity relationships (SARs) studies have investigated altering the aryl substituents to explore or reduce the lipophilicity of these series resulting in leads such as AZD9056, CE-224,535, and speculatively AFC-5128.<sup>3b, 3d</sup> Large molecular mass is a consequence of this strategy which could impede bioavailability and blood-brain penetration. The amide linker has been reversed, substituted and replaced (such as in GSK1482160) with no significant improvements reported. Early hit-to-lead studies have suggested that removing or flattening the adamantane to a simpler cycloalkane, to reduce lipophilicity and molecular weight, is detrimental to potency suggesting a large three-dimensional structure is central to potent P2X<sub>7</sub>R antagonism.<sup>5</sup> We, and others,<sup>6</sup> have confirmed this notion by substituting the adamantane of lead benzamide **1** with a variety of polycyclic cages (from cubane to carborane) and found that the larger polycyclic volume was crucial for P2X<sub>7</sub>R antagonism.<sup>3c</sup> Unfortunately, the larger polycycles also result in more lipophilic compounds. In fact, most of the potent benzamide-based P2X<sub>7</sub>R antagonists reported in the literature all appear to suffer from high lipophilicity - a consequence of having an adamantane cage. We therefore sought to explore whether the original adamantanyl

benzamide structures, identified as potent P2X<sub>7</sub>R antagonists *albeit* poor drug candidates due to high lipophilicity and poor metabolic stability, could be improved through bioisosteric strategies with the aim to develop a pre-clinical lead suitable for CNS studies. In this study, two common bioisosteric strategies were systematically explored - heteroaromatic replacement of the aryl ring and the fluorine-for-hydrogen substitution on the adamantane cage. These strategies were investigated through the synthesis and biological evaluation of a series of bioisosteres of adamantanyl benzamide **1**. Adamantanyl benzamide **1** (hP2X<sub>7</sub>R pA<sub>2</sub> 8.8) was one of the lead benzamides identified in AstraZeneca's HTS and was the basis of our previous exploration on polycycle alternatives.<sup>3c</sup> As such, this investigation would provide further systematic data to aid in the development of a P2X<sub>7</sub>R pharmacophore. Furthermore, the methoxy group has the potential to be used as a site for radio-labeling in PET imaging studies as is the case for JNJ54173717 (Figure 1).<sup>7</sup>

Our initial strategy looked at replacing the benzene ring with heteroaromatic rings, namely azabenzene and diazines, which has shown to both reduce lipophilicity and improve metabolic stability in other applications.<sup>8</sup> Three regioisomers for the pyridine analogues of lead benzamide **1** are possible (Scheme 1). The *ortho*-pyridine **2** and *para*-pyridine **3** analogues (with respect to the carboxamide) were synthesized *via* the same synthetic sequence. In each case, the pyridinyl nitrogen of 3,6-dichloropyridine **4** and 2,5-dichloropyridine **5** was exploited to regioselectively direct aromatic nucleophilic substitution of the desired chloride with methoxide in excellent yields. Amide coupling with

**Scheme 1. Synthesis of heteroaromatic analogues of benzamide 1.<sup>a</sup>**

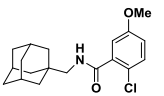
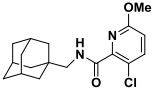
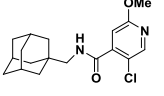
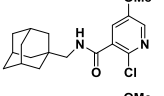
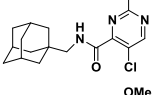
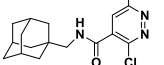


<sup>a</sup>Reaction conditions (yields in parentheses): (a) NaOMe, MeOH, sealed flask, 100 °C, 20 h; (b) (COCl)<sub>2</sub>, CH<sub>2</sub>Cl<sub>2</sub>, rt, 1 h, then 1-adamantanylmethylamine•HCl **8**, Et<sub>3</sub>N, CH<sub>2</sub>Cl<sub>2</sub>, 17 h; (c) MeI, K<sub>2</sub>CO<sub>3</sub>, DMF, rt, 20 h; (d) LiOH, MeOH/THF/H<sub>2</sub>O, rt; (e) NaOMe, MeOH, sealed flask, rt, 1 h; (f) Ethyl pyruvate, AcOH, H<sub>2</sub>O<sub>2</sub>, FeSO<sub>4</sub>, H<sub>2</sub>SO<sub>4</sub>, PhMe/H<sub>2</sub>O, <0 °C, 40 min; (g) 1-adamantanylmethylamine **8**, neat, sealed tube, 120 °C, 15 h.

adamantanylmethylamine **8** *via in situ* acid chloride formation generated the picolinamide **2** and isonicotinamide **3** analogues. The nicotinamide **9** analogue was synthesized from 2-chloro-5-hydroxynicotinic acid **10** which was alkylated to form ester **11**, then saponified to nicotinic acid **12**. Finally, amide coupling to adamantanylmethylamine **8** generated nicotinamide **9**.

To further explore the effect of heteroaromatic substitution on lead benzamide **1**, the three possible diazine regioisomers were synthesized. The pyrimidine-4-carboxamide analogue **13** was prepared from 2,5-dichloropyrimidine **14**, with the dual activation of the pyrimidine nitrogen atoms making the desired chloride substitution with methoxide regioselectively easy to generate pyrimidine **15**. The ester functionality of **16** was then installed *via* a Minisci-type reaction which required strict control of reaction time to minimize over-reaction to the diester.<sup>9</sup> Saponification of ester **16** yielded the pyrimidinecarboxylic acid which was insoluble in most solvents, making amide coupling challenging. Consequently, direct aminolysis of ester **16** with adamantanemethylamine **8** was sufficient to generate pyrimidinamide-4-carboxamide **13** for testing. The pyridazinamide **17** was synthesized in an identical route from 3,6-dichloropyridazine **18** except the pyridazinecarboxylic acid **21** was synthetically useful in generating pyridazinamide **17**. Unfortunately, the pyrazinamide analogue **22** could not be obtained from the same route. Several other synthetic means of obtaining the final diazine regioisomer **22** also proved unfruitful and so the synthesis of the pyrazinamide analogue **22** was stalled until the heteroaromatic analogues available in hand were assessed for biological activity.

**Table 1. SAR for azabenzamide series.**

Compound	LogD <sub>7.4</sub> <sup>a</sup>	IC <sub>50</sub> (nM) <sup>b</sup>	LLE <sup>c</sup>
	4.23	10.5 ± 3.1	3.75
	4.39	324 ± 78	2.10
	4.13	63.1 ± 9.4	3.07
	3.64	148 ± 25	3.19
	3.86	1410 ± 180	1.99
	4.04	2240 ± 190	1.61

<sup>a</sup> Determined experimentally by HPLC. <sup>b</sup> IC<sub>50</sub> values were the mean values (n >4) ± standard deviation derived from a dye uptake assay with THP-1 cells. <sup>c</sup> LLE = pIC<sub>50</sub> - LogD.

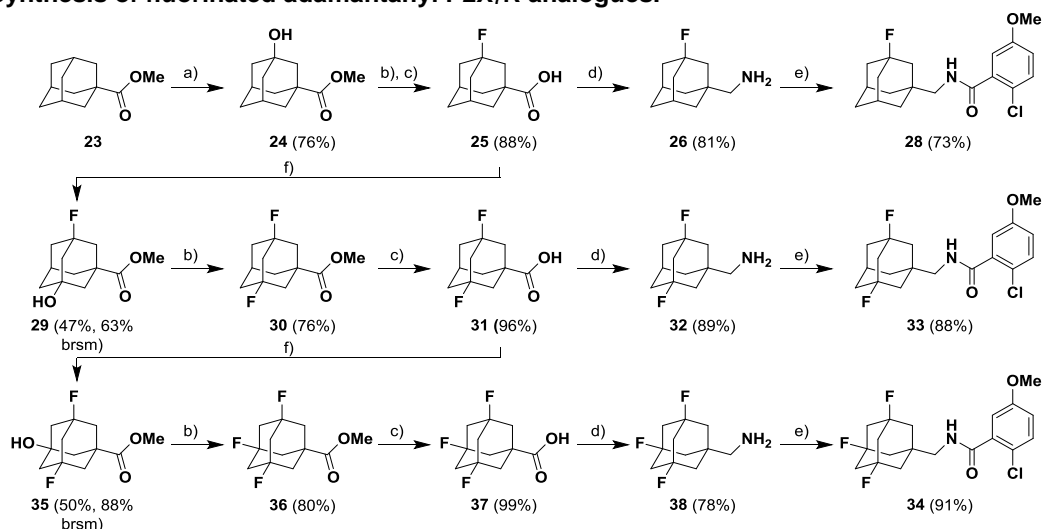
The lipophilicity of the azabenzamide series (Table 1) was evaluated by an experimentally-derived LogD<sub>7.4</sub> value determined by a HPLC method.<sup>10</sup> All analogues, except for the 2-pyridinamide **2**, were less lipophilic than lead benzamide **1**. The azabenzamide series were then assessed *in vitro* for their ability to inhibit human P2X<sub>7</sub>R (hP2X<sub>7</sub>R) pore formation by using a functional dye uptake assay in THP-1 cells.<sup>11</sup> Unexpectedly, the entire azabenzamide series was less active than lead benzamide **1** (IC<sub>50</sub> 10.5 nM) with the isonicotinamide analogue **3** being the best of the series (IC<sub>50</sub> 63.1 nM). The addition of a second nitrogen into the ring to generate the diazine series (**13** and **17**) resulted in a further reduction of activity. The micromolar potency exhibited by these two diazines suggested that the planned pyrazinamide **22** was not likely worth exploring. The Ligand-Lipophilicity Efficiency (LLE) calculated for each of the azabenzamide analogues were less than the lead benzamide **1** suggesting they are all less drug-like.<sup>12</sup> The drastic loss in P2X<sub>7</sub>R inhibition far surpassed any benefits gained by reducing the lipophilicity of lead benzamide **1** through this bioisosteric manipulation. Overall, it was observed that altering the electronics of the benzene ring of lead benzamide **1** through heteroaromatic substitution is detrimental to P2X<sub>7</sub>R inhibition and is not a viable bioisosteric strategy to apply to the benzamide P2X<sub>7</sub>R inhibitor series.

Our second bioisosteric strategy investigated the introduction of fluorine-for-hydrogen substitution at the bridgehead carbons of the adamantane cage. The highly electronegative fluorine atom forms strong, polar covalent bonds with carbon that reduces lipophilicity and blocks metabolically-labile sites. Its small atomic radius mimics the hydrogen atom to ensure no steric bulk is added to the molecule. The synthesis of the fluorinated adamantane bioisosteres replicates the synthetic strategy reported by Pfizer involving a series of oxidation and deoxyfluorination steps.<sup>13</sup>

To begin, methyl adamantanecarboxylate **23** was hydroxylated *via* a nitronium ion mediated hydride abstraction in nitric and sulfuric acid.<sup>14</sup> The subsequent hydroxyl-ester **24** was then subjected to deoxyfluorination to install the first bridgehead fluorine and then hydrolyzed to generate 3-fluoroadamantane-carboxylic acid **25** and is a divergent point of the synthesis. The 3-fluoroadamantanecarboxylic acid **25** can be converted to the 3-fluoroadamantanemethylamine **26** by amidation with ammonia then subsequent lithium aluminum hydride reduction of the carboxamide. The 3-fluoroadamantanemethylamine **26** is then coupled to the desired 2-chloro-5-methoxybenzoic acid **27** (Supporting information) with PyBOP to yield the monofluorinated benzamide analogue **28** in 73% yield. The procedure of oxidation (*albeit* with permanganate), deoxyfluorination and PyBOP coupling was repeated to obtain the 3,5-difluoro and 3,5,7-trifluoro analogs **33** and **34** respectively.

A single crystal X-ray structure of trifluorinated benzamide **34** was successfully obtained (S information) which confirms the three fluorine atoms on the bridgehead carbons of adamantane and also illustrates the *ortho* chlorine atom sterically forcing the benzamide amide bond to twist out of plane with the benzene ring (ϕ

**Scheme 2. Synthesis of fluorinated adamantanyl P2X<sub>7</sub>R analogues.<sup>a</sup>**



<sup>a</sup>Reaction conditions (yields in parentheses): (a) HNO<sub>3</sub>, H<sub>2</sub>SO<sub>4</sub>, 4-30 °C, 2 h, then EtOAc/H<sub>2</sub>O, (NH<sub>2</sub>)<sub>2</sub>CO, 4 °C to RT, 4 h, 76%; (b) Deoxyfluor, CHCl<sub>3</sub>, -78 °C to reflux, 2 h; (c) NaOH, MeOH, Δ, 4 h; (d) (i) CDI, THF, rt, 1 h then NH<sub>4</sub>OH<sub>(aq)</sub>, rt, 4 h; (ii) LiAlH<sub>4</sub>, THF, Δ, 21 h; (e) 2-chloro-5-methoxybenzoic acid **27**, PyBOP, DIPEA, CH<sub>2</sub>Cl<sub>2</sub>, 18 h; (f) (i) KMnO<sub>4</sub>, KOH, H<sub>2</sub>O, Δ, 2-21 h, then HCl; (ii) H<sub>2</sub>SO<sub>4</sub>, MeOH, Δ, 2h.

39°) which several groups have speculated as being an important pharmacophore of the benzamide series.<sup>15</sup> Indeed, the synthesis to install fluorine-for-hydrogen substitution on the adamantane cage proved to be valuable with the HPLC-determined LogD<sub>7.4</sub> values (Table 2) for all fluorinated analogues reported to be less than the lead benzamide **1** and the azabenzamide series (Table 1). The fluorinated benzamides **28**, **33**, and **34** still displayed nanomolar activity in the hP2X<sub>7</sub>R functional assay and other *in vitro* assays. Only a small reduction in activity resulted from the installation of the fluorine atoms suggesting the fluorine-for-hydrogen substitution on the

adamantane cage is tolerated. With reduced lipophilicity and comparable P2X<sub>7</sub>R activity relative to the lead benzamide **1**, these fluorinated benzamides exhibited much higher LLE values than the lead benzamide **1** suggesting they may be improved drug candidates.

A molecular hybrid of the two bioisosteric studies was also synthesized to validate the trends observed in both these studies. The 3,5-difluoro isonicotinamide **39** was synthesized from the amide coupling of 3,5-difluoroadamantanemethylamine **32** and 5-chloro-2-methoxyisonicotinic acid **7**. The isonicotinic acid **7** was

**Table 2. SAR for the fluorinated adamantanylbenzamide series.**

Compound	LogD <sub>7.4</sub>	Dye uptake IC <sub>50</sub> hP2X <sub>7</sub> R (nM) <sup>a</sup>	Calcium influx IC <sub>50</sub> (nM) <sup>b</sup> hP2X <sub>7</sub> R	mP2X <sub>7</sub> R	Binding affinity K <sub>i</sub> (nM) <sup>c</sup>	LLE <sup>d</sup>	
	<b>1</b>	4.23	10.5 ± 3.1	25.7 ± 8.7	1905 ± 905	8.5 ± 0.6	3.75
	<b>28</b>	3.27	25.1 ± 2.7	17.4 ± 2.9	1513 ± 339	21.9 ± 0.5	4.33
	<b>33</b>	2.85	30.9 ± 8.0	10.0 ± 4.0	575 ± 108	23 ± 5	4.66
	<b>34</b>	2.83	33.9 ± 11	24.5 ± 5.5	158 ± 44	32 ± 5	4.64
	<b>39</b>	2.82	234 ± 30	-	-	-	3.81

<sup>a</sup> IC<sub>50</sub> values were the mean values (n > 4) ± standard deviation derived from a dye uptake assay with THP-1 cells. <sup>b</sup> IC<sub>50</sub> values were the mean values (n > 3) ± standard deviation derived from calcium influx in HEK cells expressing hP2X<sub>7</sub>R or mP2X<sub>7</sub>R. <sup>c</sup> Binding affinities (K<sub>i</sub>) were the mean values (n > 3) ± standard deviation derived from the displacement of tritium-labeled benzamide **1-3** in HEK cells expressing hP2X<sub>7</sub>R. <sup>d</sup> LLE = pIC<sub>50</sub> (from dye uptake) – LogD (from HPLC). Details of all assay conditions are provided in the Supporting Information.

selected for the study as its azabenzamide resulted in the highest activity (IC<sub>50</sub> 63 nM) of the azabenzamide series. The two bioisosteric strategies had a synergistic effect on lipophilicity with the hybrid benzamide **39** possessing the lowest lipophilicity of our entire library (LogD<sub>7.4</sub> 2.82). Unfortunately, the loss in hP2X<sub>7</sub>R activity of each bioisostere also appeared to coalesce to produce a molecular hybrid with less activity (IC<sub>50</sub> 234 nM) than each of the individual bioisosteres **33** (IC<sub>50</sub> 30.9 nM) and **3** (IC<sub>50</sub> 63 nM) and much less than the lead benzamide **1** (IC<sub>50</sub> 10.5 nM).

Based on these results, fluorinated benzamides **28**, **33**, and **34** were progressed further. The hP2X<sub>7</sub>R inhibition activity of the lead benzamide **1** and fluorinated benzamides **28**, **33**, and **34** were evaluated further by a calcium influx assay (Table 2). In this assay, all the fluorinated benzamides exhibited a greater inhibitory effect (IC<sub>50</sub> 10-25 nM) than in the dye uptake assay (IC<sub>50</sub> 25-34 nM). In addition, these results were equal to or better than the lead benzamide **1** (IC<sub>50</sub> 26 nM). Interestingly, the activity of the lead benzamide **1** and all three fluorinated analogues **28**, **33**, and **34** in the mP2X<sub>7</sub>R calcium flux assay was particularly poor. Whilst all benzamides perform equally well on the hP2X<sub>7</sub>R, there appears to be a trend with the mP2X<sub>7</sub>R favoring the more fluorinated benzamides. The reduced activity of the benzamides on the mP2X<sub>7</sub>R was not unexpected given the adamantanyl benzamide series are allosteric inhibitors and so likely possess poor interspecies crossover.<sup>15</sup> Nevertheless, the trifluorobenzamide **34** only exhibits a 6-fold drop in activity against the mP2X<sub>7</sub>R, compared to a 74-fold drop for the desfluorobenzamide **1**, and so may be a useful probe in evaluating the role of the P2X<sub>7</sub>R in mouse disease models.

The tritium radiolabeled parent benzamide (**1-t<sub>3</sub>**) was used to examine the binding affinities of the fluorinated benzamide analogues on membranes from human P2X<sub>7</sub>R HEK-transfected cells (Table 2). All fluorinated benzamides exhibited comparative binding affinities (22-32 nM) to the parent benzamide (8.5 nM). There was a slight drop in affinity with the addition of each fluorine atom to the adamantane cage suggesting the adamantane cage plays a critical role in binding to a hydrophobic pocket which is subtly disrupted, yet tolerated, with the addition of each electronegative fluorine atom.

With the fluorinated bioisosteres **28**, **33** and **34** demonstrating improved drug-like properties over lead benzamide **1** in pharmacological studies, they were progressed to *in vitro* drug metabolism studies (Table 3). None of the fluorinated benzamides were identified as potential P-gp substrates in apparent permeability studies with all compounds exhibiting similar efflux ratios. This is a promising result given that AZD9056, a closely-related adamantane benzamide that failed in phase IIb clinical trials, is reported as being a P-gp substrate.<sup>16</sup>

In rat liver microsome (RLM) stability studies, the addition at least 2 fluorine atoms to the adamantane cage was required to note any improvement in compound half-life. The trifluorobenzamide **34** exhibited the greatest stability with a half-life 6 times longer than the lead benzamide **1**. A similar trend is observed in the CYP profile studies whereby the fluorinated benzamides **28**, **33** and

**34** encountered less CYP enzyme interactions (with the exception of CP3A4) than the lead benzamide **1** with the trifluorinated benzamide **34** performing the best. Future studies will assess the extent of CYP3A4 inhibition at the lower concentrations envisaged for dosing. The oxidation of the bridgehead carbons of adamantane is a major metabolic pathway for adamantane<sup>17</sup> and we speculate that this is the likely fate for all conventional adamantanyl benzamide libraries which ultimately translates to poor pharmacokinetic results. Through the fluorination of the bridgehead carbons of the adamantane moiety, we have not only improved the physicochemical properties of lead benzamide **1**, but also hindered the main metabolic pathway which has resulted in metabolically more stable compounds.

**Table 3. Metabolism data for fluorinated benzamides.**

		<b>1</b>	<b>28</b>	<b>33</b>	<b>34</b>
<b>P<sub>app</sub><sup>a</sup></b> <b>(x10<sup>-6</sup> cm/sec)</b>	<b>A-B</b>	40.9	28.1	40.0	30.3
	<b>B-A</b>	23.6	34.3	54.8	44.2
<b>Liver microsome<sup>b</sup> T<sub>1/2</sub> (h)</b>		0.13	0.08	0.30	0.78
	<b>1A2</b>	25.68	7.86	7.04	5.48
<b>CYP Profiling<sup>c</sup></b> <b>(% inhibition with</b> <b>10 μM substrate)</b>	<b>2C9</b>	74.97	32.33	-3.00	9.26
	<b>2C19</b>	84.43	46.91	1.50	12.90
	<b>2D6</b>	-47.26	-28.95	-25.29	-29.14
	<b>3A4</b>	84.43	88.75	89.88	89.93

<sup>a</sup> P<sub>app</sub> values were mean values (n=3) ± standard deviation derived from bi-directional transcellular permeability assay using Madin-Darby canine kidney (MDCK) cells. <sup>b</sup> Half-lives were calculated using the gradient derived from plotting compound stability against time with n=3 at each time point. <sup>c</sup> Cytochrome P450 isozyme inhibition values were mean (n=3) ± SEM. Details of all assay conditions are provided in the Supporting Information.

One of the major challenges that this study seeks to address is to improve the pharmacokinetic profile of lead benzamide **1**, which was reported to have poor bioavailability following oral administration. Whilst the mono and difluorinated benzamides **28** and **33** respectively, exhibited similar pharmacokinetics to the lead benzamide **1**, the trifluorinated benzamide **34** displayed superior results (Table 4). All four compounds achieved equivalent maximum concentrations (C<sub>max</sub> 4-7 mM) in the brain that equated to over 100 times their binding affinity (Table 2). However, all three fluorinated benzamides exhibited a higher percentage of unbound drug, in both plasma and brain, than lead benzamide **1**. In the brain, the distribution of benzamides increases proportional to the amount of fluorine atoms present on adamantane with the volume of distribution (V<sub>d</sub>) for trifluorobenzamide **34** determined to be 3 times greater than lead benzamide **1**. Analyzing the elimination data, we observe that trifluorobenzamide **34** exhibits enhanced metabolic stability over all other benzamides of the series [consistent with our RLM results (Table 3)], with a plasma and brain half-life (T<sub>1/2</sub>) of 3.7 and 7.9 (respectively) times longer than the lead benzamide **1**. The improved metabolic stability of trifluorobenzamide **34** resulted in an improved drug exposure profile (AUC) which was almost twice that of all other benzamides in the series.

**Table 4. Pharmacokinetic data for the fluorinated benzamide series in rats.**

Tissue	1		28		33		34	
	Plasma	Brain	Plasma	Brain	Plasma	Brain	Plasma	Brain
pb <sup>a</sup> (%bound)	99.21	99.73	94.03	96.91	88.46	91.50	89.53	94.51
T <sub>1/2</sub> (h)	0.47	0.16	0.43	0.43	0.47	0.59	1.72	1.26
T <sub>max</sub> (h)	0.02	0.02	0.02	0.02	0.02	0.02	0.02	0.02
C <sub>max</sub> (ng/mL)	1190	1696	1265	2422	1716	1838	1289	1464
AUC <sub>6</sub> (h*ng/mL)	185.97	221.46	174.99	286.32	195.53	209.02	385.01	380.46
AUC <sub>∞</sub> (h*ng/mL)	191.79	245.91	178.42	290.73	199.49	216.77	398.64	385.56
Cl (mL/min/kg)	86.90	67.78	93.41	57.33	83.55	76.89	41.81	43.23
V <sub>d</sub> (L/kg)	2.09	0.77	1.80	0.92	1.41	1.54	2.75	2.10

<sup>a</sup> Brain and plasma protein binding values were mean (n=3) ± SEM with tissue and blood pooled from rats. Details of all assay conditions are provided in the Supporting Information.

In humans, the P2X<sub>7</sub>R is highly polymorphic with the current Build of the NCBI database (Build 141) reporting 299 amino acid altering mutations in hP2X<sub>7</sub>R, of which 11 have a minor allele frequency above 1% (defined as a single nucleotide polymorphism; SNP). Many studies are linking P2RX<sub>7</sub>R polymorphisms to various disease states.<sup>18</sup> It is therefore imperative that any potential drug lead also be effective against disease-inducing polymorphisms. We explored the inhibitory potency of our trifluorinated benzamide **34** lead against six functionally characterized hP2X<sub>7</sub>R SNPs which are known to cause either gain-of-function or no change in function of hP2X<sub>7</sub>R (Table 5). The trifluorinated benzamide **34** is well tolerated against these SNPs with little to no loss of inhibitory activity, suggesting a potential to modulate P2X<sub>7</sub>R activity in diseases states involving polymorphisms.

**Table 5. Activity of trifluorobenzamide 34 in the presence of hP2X<sub>7</sub>R SNPs.**

AA Change	Frequency <sup>19</sup>	% WT Function	IC <sub>50</sub> (nM) <sup>a</sup>	
			1 mM ATP	100 μM BzATP
WT			49 ± 24	33 ± 6
V76A	0.062	44% <sup>19</sup>	ND	24 ± 9
H155T	0.439	195% <sup>19</sup>	49 ± 21	20 ± 5
H270R	0.255	195% <sup>19</sup>	34 ± 17	52 ± 20
A348T	0.400	>100% <sup>20</sup>	48 ± 6	30 ± 10
T357S	0.083	41% <sup>21</sup>	ND	35 ± 12
Q460R	0.170	73%	55 ± 4 <sup>b</sup>	62 ± 16 <sup>b</sup>

<sup>a</sup> IC<sub>50</sub> values were the mean values (n = 2-3 transfections) ± standard deviation derived from a dye uptake assay against ATP (1 mM) or BzATP (100 μM) with HEK293 cells transiently transfected with plasmids of functional P2X<sub>7</sub>R SNP variants. <sup>b</sup> Plasmid contains 348T and 460R.

We describe the synthesis, SAR and pharmacokinetic results of a series of azabenzamide and fluorinated adamantane bioisosteres of lead benzamide **1** in an effort to improve the lead's physicochemical and pharmacokinetic properties. Incorporation of one or two nitrogen atoms into the benzene ring, to generate the azabenzamide series, resulted in less lipophilic candi-

dates but at the expense of significantly reduced inhibition values. Incorporation of fluorine at the bridgehead carbons of the adamantane moiety was well tolerated with a slight loss of P2X<sub>7</sub>R inhibition activity yet significantly improved physicochemical and PK properties compared to lead benzamide **1**. The fluorinated benzamide series have also provided insight into poor metabolic stability of lead benzamide **1**. Through the installation of fluorine on the adamantane bridgeheads, we have blocked the common oxidation sites of adamantane and enhanced the metabolic stability of the benzamide series. The most promising candidate of this study is trifluorinated benzamide **34** which demonstrated potent P2X<sub>7</sub>R inhibition, a strong reduction in lipophilicity, improved PK properties (particularly in metabolic stability and CYP profiling) and was effective across several polymorphs of the hP2X<sub>7</sub>R. Future studies endeavor to utilize the trifluorobenzamide **34** to test the effects of P2X<sub>7</sub>R antagonism in pre-clinical models of CNS disorders and as a suitable PET radiotracer.

## ASSOCIATED CONTENT

Synthesis, characterization (including X-ray crystal data), and biological assays. This material is available free of charge via the Internet at <http://pubs.acs.org>.

## AUTHOR INFORMATION

### Corresponding Author

\* M.K. Telephone: +61 2 9351 2745. Fax: +61 2 9351 3329. Email: [michael.kassiou@sydney.edu.au](mailto:michael.kassiou@sydney.edu.au).

### Author Contributions

The manuscript was written through contributions of all authors. All authors have given approval to the final version of the manuscript. S.M.W. synthesized benzamides **1**, **28**, **33** and **34** and prepared drafts of this article. J.O.B. synthesized benzamides **2**, **3**, **9**, **13**, **17**, and **39**. M.L.B. performed the functional cell assays (dye uptake and calcium influx) and the binding studies. L.S. generated P2X<sub>7</sub> cell lines used in the study. E.W. assisted in the development of the calcium influx assays, radioligand binding, and manuscript editing. M.C. performed the pharmacokinetic studies. K.K.S. carried out the SNPs studies under the supervision of S.F. J.A.G. resolved and catalogued the X-ray crystal structure of benzamide **34** under the supervision of D.E.H. B.J. syn-

thesized the tritium benzamide. D.J.V. and A.D.W. supervised part of the project while M.K. conceived this project and directed the synthesis and *in vitro* work.

### Funding Sources

The work presented herein was supported in part by NH&MRC and the European Union's Seventh Framework Programme [FP7/2007-2013] INMiND (Grant Agreement No. HEALTH-F2-2011-278850).

### Notes

The authors declare no competing financial interest.

### ACKNOWLEDGMENT

We wish to acknowledge Dr. Donna Lai and Dr. Sheng Hua (Bosch Molecular Biology Facility, Sydney University) for assistance with use of the Bosch Molecular Biology Facility's equipment. The work presented herein was supported in part by NH&MRC and the European Union's Seventh Framework Programme [FP7/2007-2013] INMiND (Grant agreement No. HEALTH-F2-2011-278850).

### ABBREVIATIONS

CNS, central nervous system; P2X<sub>7</sub>R, purinergic 2X subtype 7 receptor; PK, pharmacokinetics.

### REFERENCES

1. Bartlett, R.; Stokes, L.; Sluyter, R., The P2X<sub>7</sub> Receptor Channel: Recent Developments and the Use of P2X<sub>7</sub> Antagonists in Models of Disease. *Pharmacol. Rev.* **2014**, *66* (3), 638-675.
2. (a) Carroll, W. A.; Donnelly-Roberts, D.; Jarvis, M. F., Selective P2X<sub>7</sub> receptor antagonists for chronic inflammation and pain. *Purinergic Signal.* **2009**, *5* (1), 63-73; (b) Hendra, G.; Mark, J. C.; Michael, K., Molecular Probes for P2X<sub>7</sub> Receptor Studies. *Curr. Med. Chem.* **2007**, *14* (14), 1505-1523.
3. (a) Park, J.-H.; Kim, Y.-C., P2X<sub>7</sub> receptor antagonists: a patent review (2010–2015). *Expert Opin. Ther. Pat.* **2017**, *27* (3), 257-267; (b) Furber, M.; Alcaraz, L.; Bent, J. E.; Beyerbach, A.; Bowers, K.; Braddock, M.; Caffrey, M. V.; Cladingboel, D.; Collington, J.; Donald, D. K.; Fagura, M.; Ince, F.; Kinchin, E. C.; Laurent, C.; Lawson, M.; Luker, T. J.; Mortimore, M. M. P.; Pimm, A. D.; Riley, R. J.; Roberts, N.; Robertson, M.; Theaker, J.; Thorne, P. V.; Weaver, R.; Webborn, P.; Willis, P., Discovery of Potent and Selective Adamantane-Based Small-Molecule P2X<sub>7</sub> Receptor Antagonists/Interleukin-1 $\beta$  Inhibitors. *J. Med. Chem.* **2007**, *50* (24), 5882-5885; (c) Wilkinson, S. M.; Gunosewoyo, H.; Barron, M. L.; Boucher, A.; McDonnell, M.; Turner, P.; Morrison, D. E.; Bennett, M. R.; McGregor, I. S.; Rendina, L. M.; Kassiou, M., The First CNS-Active Carborane: A Novel P2X<sub>7</sub> Receptor Antagonist with Antidepressant Activity. *ACS Chem. Neurosci.* **2014**, *5* (5), 335-339; (d) Keystone, E. C.; Wang, M. M.; Layton, M.; Hollis, S.; McInnes, I. B., Clinical evaluation of the efficacy of the P2X<sub>7</sub> purinergic receptor antagonist AZD9056 on the signs and symptoms of rheumatoid arthritis in patients with active disease despite treatment with methotrexate or sulphasalazine. *Annals of the rheumatic diseases* **2012**, *71* (10), 1630-1635.
4. Baxter, A.; Bent, J.; Bowers, K.; Braddock, M.; Brough, S.; Fagura, M.; Lawson, M.; McInally, T.; Mortimore, M.; Robertson, M.; Weaver, R.; Webborn, P., Hit-to-Lead studies: The discovery of potent adamantane amide P2X<sub>7</sub> receptor antagonists. *Bioorg. Med. Chem. Lett.* **2003**, *13* (22), 4047-4050.
5. Evans, R.; Eyssade, C.; Ford, R.; Martin, B.; Thompson, T.; Willis, P. Preparation of quinolyl amides as new P2X<sub>7</sub> receptor antagonists. WO2004106305A1, 2004.
6. Barniol-Xicota, M.; Kwak, S.-H.; Lee, S.-D.; Caseley, E.; Valverde, E.; Jiang, L.-H.; Kim, Y.-C.; Vázquez, S., Escape from adamantane: Scaffold optimization of novel P2X<sub>7</sub> antagonists featuring complex polycycles. *Bioorg. Med. Chem. Lett.* **2017**, *27* (4), 759-763.
7. Ory, D.; Celen, S.; Gijsbers, R.; Van Den Haute, C.; Postnov, A.; Koole, M.; Vandeputte, C.; Andrés, J.-I.; Alcazar, J.; De Angelis, M.; Langlois, X.; Bhattacharya, A.; Schmidt, M.; Letavic, M. A.; Vanduffel, W.; Van Laere, K.; Verbruggen, A.; Debyser, Z.; Bormans, G., Preclinical Evaluation of a P2X<sub>7</sub> Receptor-Selective Radiotracer: PET Studies in a Rat Model with Local Overexpression of the Human P2X<sub>7</sub> Receptor and in Nonhuman Primates. *Journal of Nuclear Medicine* **2016**, *57* (9), 1436-1441.
8. Meanwell, N. A., Synopsis of Some Recent Tactical Application of Bioisosteres in Drug Design. *J. Med. Chem.* **2011**, *54* (8), 2529-2591.
9. Regan, C. F.; Pierre, F.; Schwaebe, M. K.; Haddach, M.; Jung, M. E.; Ryckman, D. M., A facile synthesis of 5-halopyrimidine-4-carboxylic acid esters via a Minisci reaction. *Synlett* **2012**, *2012* (03), 443-447.
10. Haky, J. E.; Young, A. M., Evaluation of a Simple HPLC Correlation Method for the Estimation of the Octanol-Water Partition Coefficients of Organic Compounds. *J. Liq. Chromatogr.* **1984**, *7* (4), 675-689.
11. Donnelly-Roberts, D. L.; Namovic, M. T.; Han, P.; Jarvis, M. F., Mammalian P2X<sub>7</sub> receptor pharmacology: comparison of recombinant mouse, rat and human P2X<sub>7</sub> receptors. *Br. J. Pharmacol.* **2009**, *157* (7), 1203-1214.
12. Hopkins, A. L.; Keseru, G. M.; Leeson, P. D.; Rees, D. C.; Reynolds, C. H., The role of ligand efficiency metrics in drug discovery. *Nat Rev Drug Discov* **2014**, *13* (2), 105-121.
13. Jasys, V. J.; Lombardo, F.; Appleton, T. A.; Bordner, J.; Ziliox, M.; Volkmann, R. A., Preparation of Fluoroadamantane Acids and Amines: Impact of Bridgehead Fluorine Substitution on the Solution- and Solid-State Properties of Functionalized Adamantanes. *Journal of the American Chemical Society* **2000**, *122* (3), 466-473.
14. Olah, G. A.; Ramaiah, P.; Rao, C. B.; Sandford, G.; Golam, R.; Trivedi, N. J.; Olah, J. A., Electrophilic reactions at single bonds. 25. Nitration of adamantane and diamantane with nitronium tetrafluoroborate. *J. Am. Chem. Soc.* **1993**, *115* (16), 7246-7249.
15. Guile, S. D.; Alcaraz, L.; Birkinshaw, T. N.; Bowers, K. C.; Ebdon, M. R.; Furber, M.; Stocks, M. J., Antagonists of the P2X<sub>7</sub> Receptor. From Lead Identification to Drug Development. *J. Med. Chem.* **2009**, *52* (10), 3123-3141.
16. AstraZeneca AZD9056. <https://openinnovation.astrazeneca.com/azd9056.html>.
17. Wanka, L.; Iqbal, K.; Schreiner, P. R., The Lipophilic Bullet Hits the Targets: Medicinal Chemistry of Adamantane Derivatives. *Chem. Rev. (Washington, DC, U. S.)* **2013**, *113* (5), 3516-3604.
18. (a) Gu, B. J.; Field, J.; Dutertre, S.; Ou, A.; Kilpatrick, T. J.; Lechner-Scott, J.; Scott, R.; Lea, R.; Taylor, B. V.; Stankovich, J.; Butzkueven, H.; Gresle, M.; Laws, S. M.; Petrou, S.; Hoffjan, S.; Akkad, D. A.; Graham, C. A.; Hawkins, S.; Glaser, A.; Bedri, S. K.; Hillert, J.; Matute, C.; Antiguada, A.; Wiley, J. S.; Baxter, A. G.; Kermode, A. G.; Taylor, B. V.; Booth, D. R.; Mason, D. F.; Stewart, G. J.;

- Butzkueven, H.; Charlesworth, J. C.; Wiley, J. S.; Lechner-Scott, J. S.; Field, J.; Tajouri, L.; Griffiths, L. R.; Slee, M.; Brown, M. A.; Moscato, P.; Scott, R. J.; Broadley, S. A.; Vucic, S.; Kilpatrick, T. J.; Carroll, W. M.; Barnett, M. H., A rare P2X<sub>7</sub> variant Arg307Gln with absent pore formation function protects against neuroinflammation in multiple sclerosis. *Hum. Mol. Genet.* **2015**, *24* (19), 5644-5654; (b) Gartland, A.; Skarratt, K. K.; Hocking, L. J.; Parsons, C.; Stokes, L.; Jorgensen, N. R.; Fraser, W. D.; Reid, D. M.; Gallagher, J. A.; Wiley, J. S., Polymorphisms in the P2X<sub>7</sub> receptor gene are associated with low lumbar spine bone mineral density and accelerated bone loss in post-menopausal women. *Eur. J. Hum. Genet.* **2012**, *20* (5), 559-564.
19. Stokes, L.; Fuller, S. J.; Sluyter, R.; Skarratt, K. K.; Gu, B. J.; Wiley, J. S., Two haplotypes of the P2X<sub>7</sub> receptor containing the Ala-348 to Thr polymorphism exhibit a gain-of-function effect and enhanced interleukin-1 $\beta$  secretion. *FASEB J.* **2010**, *24* (8), 2916-2927.
20. Sun, C.; Chu, J.; Singh, S.; Salter, R. D., Identification and characterization of a novel variant of the human P2X<sub>7</sub> receptor resulting in gain of function. *Purinergic Signal.* **2010**, *6* (1), 31-45.
21. Shemon, A. N.; Sluyter, R.; Fernando, S. L.; Clarke, A. L.; Dao-Ung, L. P.; Skarratt, K. K.; Saunders, B. M.; Tan, K. S.; Gu, B. J.; Fuller, S. J.; Britton, W. J.; Petrou, S.; Wiley, J. S., A Thr357 to Ser polymorphism in homozygous and compound heterozygous subjects causes absent or reduced P2X<sub>7</sub> function and impairs ATP-induced mycobacterial killing by macrophages. *J Biol Chem* **2006**, *281* (4), 2079-86.
-